Electronic Supplementary Material (ESI) for ChemComm.

Supporting information

Imine-riched polymer with enlarged π-conjugated planes for aqueous zinc-ion battery

Yaxin Liang, Yuanhao Xia, Xinlei Wang, Jie Zhou*

Experimental Section

Materials

3,3'-Diaminobenzidine (DAB) was purchased from Shanghai Bide Pharmaceutical Technology Co. Ltd. Hexaketocyclohexane octahydrate ($C_6O_6 \cdot 8H_2O$) was purchased from Beijing Yinuokai Technology Co. Ltd. 2,5-Dihydroxy-1,4-benzoquinone (DHBQ) was purchased from Shanghai Merrier Biochemical Technology Co. Ltd. Deoxygenated N-methyl-2-pyrrolidone (NMP) was purchased from Shanghai Aladdin Biochemical Technology Co. Ltd. H_2SO_4 was purchased from Sinopharm Group Chemical reagent Co. Ltd. Titanium foil (diameter: 15 mm, thickness: 0.1 mm) was purchased from Guangzhou Haiyuan Metal Products Co. Ltd. Conductive carbon black (Super P Li) was purchased from Guangdong Candlelight New Energy Technology Co. Ltd. Polyvinylidene fluoride (PVDF) was purchased from Wuyu Chemical Industry Co. Ltd. Glass fiber membrane (GF/D grade) was provided by Whatman company. Zinc foil (diameter: 15 mm, thickness: 0.3 mm) was purchased from Dongguan Keloude Experimental Materials Technology Co. Ltd. Zinc sulfate heptahydrate ($ZnSO_4 \cdot 7H_2O$) was purchased from Beijing Yinuokai Technology Co. Ltd.

Synthesis of P3Q and TDB

P3Q: $C_6O_6 \cdot 8H_2O$ (0.9713 g, 3.11 mmol) and DAB (1g, 4.66 mmol) were added into a two-neck round-bottom flask under nitrogen flow and cooled in an ice bath. NMP (26 mL) with eleven drops of sulfuric acid was slowly added. The reaction mixture was warmed to room temperature over 3 h, before being transferred to an oil bath and heated to 60 °C for 12 h. Then, after cooling to room temperature, the mixture was filtered and washed by ethyl alcohol, deionized water, and acetone for several times. The obtained dark-brown solid was dried overnight at 60°C in vacuum to afford the title product (P3Q, 1.2118g yield: 91.2%).

TDB: DHBQ (0.6538 g, 4.67 mmol) and DAB (1 g, 4.67 mmol) were added into a two-neck round-bottom flask under nitrogen flow and cooled in an ice bath. NMP (39 mL) with sixteen drops of sulfuric acid was slowly added. The reaction mixture was warmed to room temperature over 3 h, before being transferred to an oil bath and heated to 60 °C for 12 h. Then, after cooling to room temperature, the mixture was filtered and washed by ethyl alcohol, deionized water, and acetone for several times. The obtained dark-brown solid was dried overnight at 60°C in vacuum to afford the

title product (TDB, 1.3018g yield: 89.2%).

Characterizations

The crystal structure of the sample was obtained by the radiation X-ray diffractometer (XRD, Japan Science, SmartLab3), and the fourier infrared spectrum (FTIR) came from the infrared spectrometer (ThermoFisher Nicolet iS-10). Solid state ^{13}C cross-polarization magic angle spinning NMR (CP/MAS NMR) spectra were taken on Bruker AVANCE NEO 400 WB spectrometer (Bruker BioSpin AG, Switzerland) spectrometer. X-ray photoelectron spectroscopy (XPS) analysis was performed on the Thermo ESCALAB 250 X-ray photoelectron spectrometer. Scanning electron microscopy (SEM) and energy dispersive X-ray spectroscopy (EDS) mapping images of the samples were obtained by J Hitachi S-4800 instrument equipped with an EDS (AMETEK) analyzer at an accelerated voltage of 3 kV. Transmission electron microscope (TEM) mapping images of the samples were obtained by FEI Talos F200X (Bruker Super-x EDS). TGA was conducted on TGA/SDTA851E (Mettler Toledo) and Raman spectra were recorded on horiba evolution. All cyclic voltammetric tests (CV) were obtained using CHI760E electrochemical workstation (Chenhua, Shanghai, China). The constant current charge/discharge (GCD) test with voltage range of 0.1V to 1.6 V was conducted on LAND CT2001A (5 V/5 mA). Theoretical simulation and calculation were based on DFT with the B3LYP/6-31G (d, p) basis set. The solvation effect using implicit solvation model for a precise simulation of the experimental conditions in water solution was also considered in the optimization.

Battery fabrication

Samples (P3Q or TDB) are mixed with Super P Li and PVDF at the ratio of 6:3:1, then NMP is added and fully milled, the resulting slurry is coated on titanium foil, and dried in vacuum at 80 °C for 12 hours. The average mass loading is kept in the range of 1.3-1.7 mg cm^{-2}. The CR2032 button battery is used, and the assembly process is in air atmosphere (Zinc foil as anode; glass fiber as separator), with 2 M ZnSO4 as aqueous electrolyte.

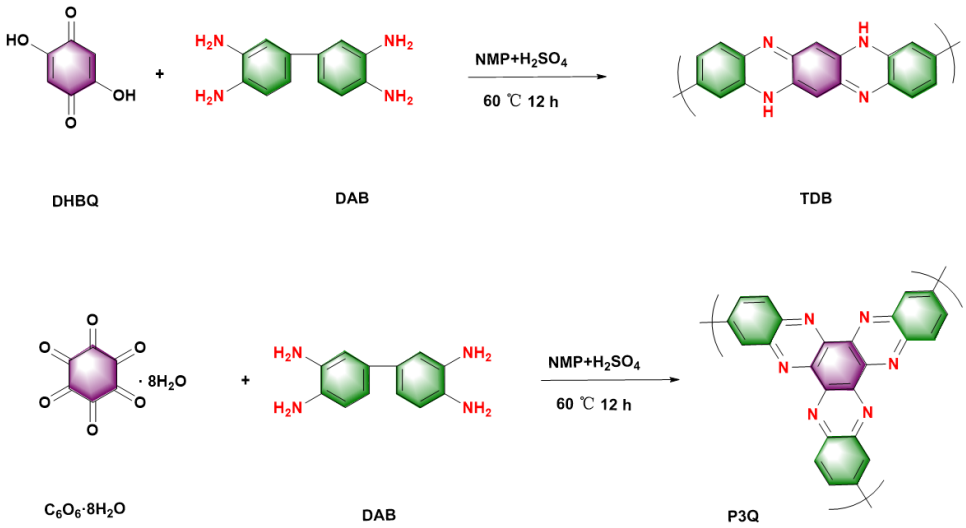

Fig S1 The synthetic procedures of TDB and P3Q.

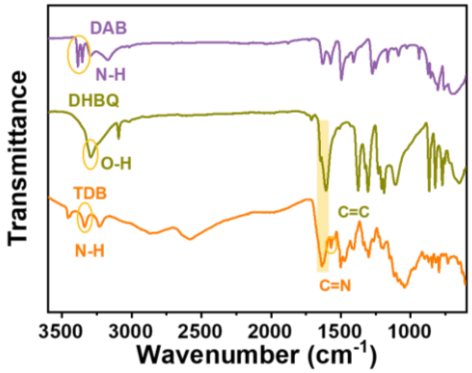

Fig S2 FT-IR spectra of DAB, DHBQ and TDB.

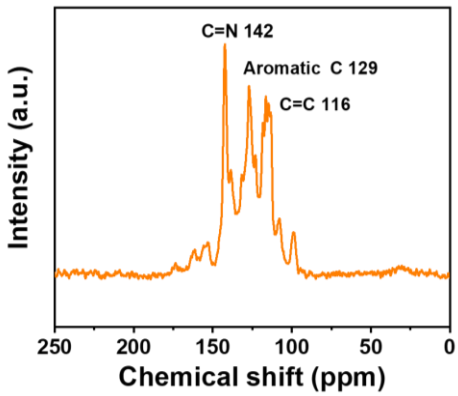

Fig S3 Solid-state ^{13}C NMR spectra of TDB.

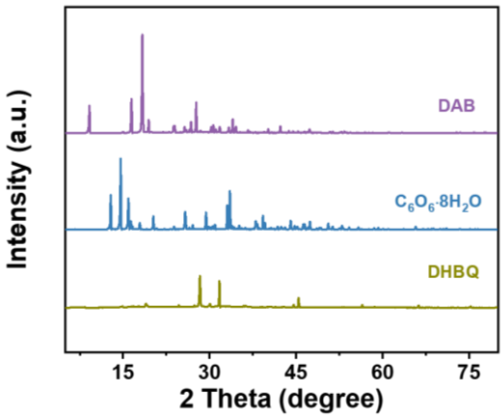

Fig S4 XRD curves of DAB, $C_6O_6 \cdot 8H_2O$ and DHBQ.

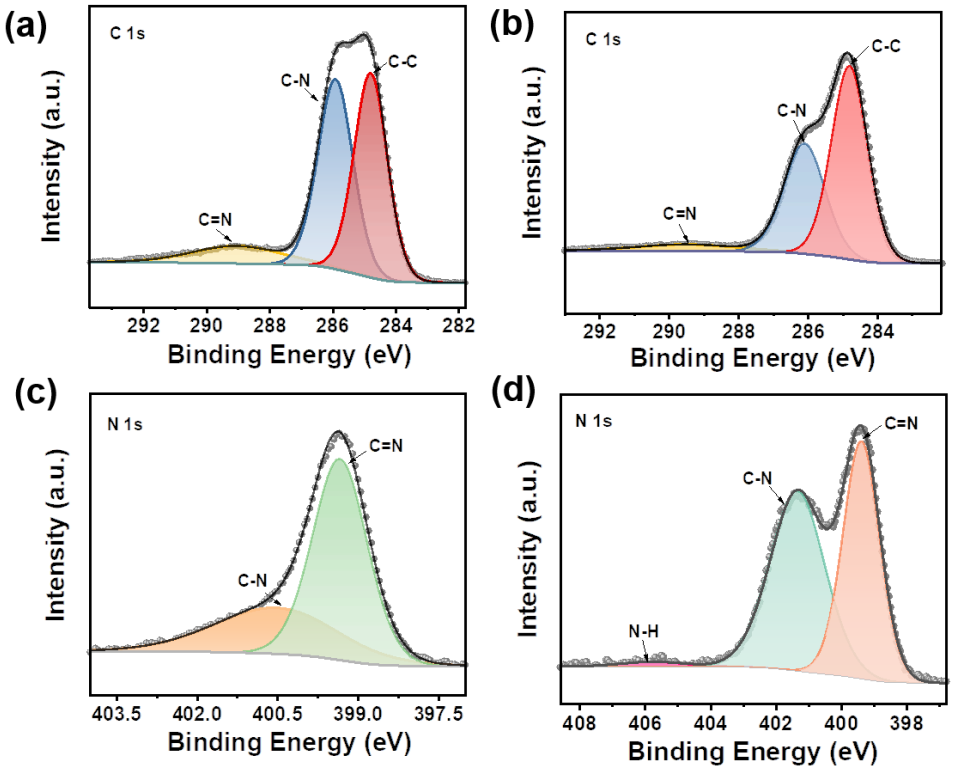

Fig S5 High-resolution XPS spectra of (a) C 1s and (c) N 1s for P3Q and (b) C 1s and (d) N 1s for TDB.

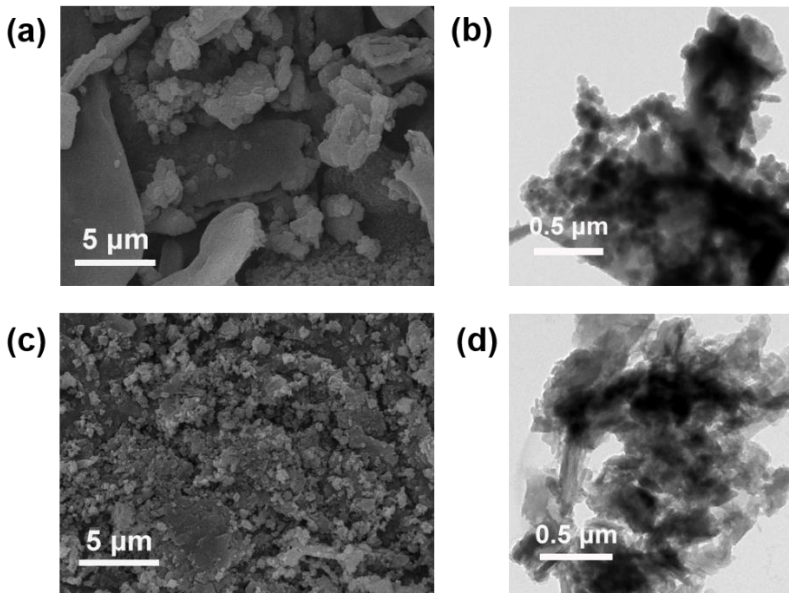

Fig S6 The SEM images of (a) P3Q and (c) TDB and TEM images of (b) P3Q and (d) TDB.

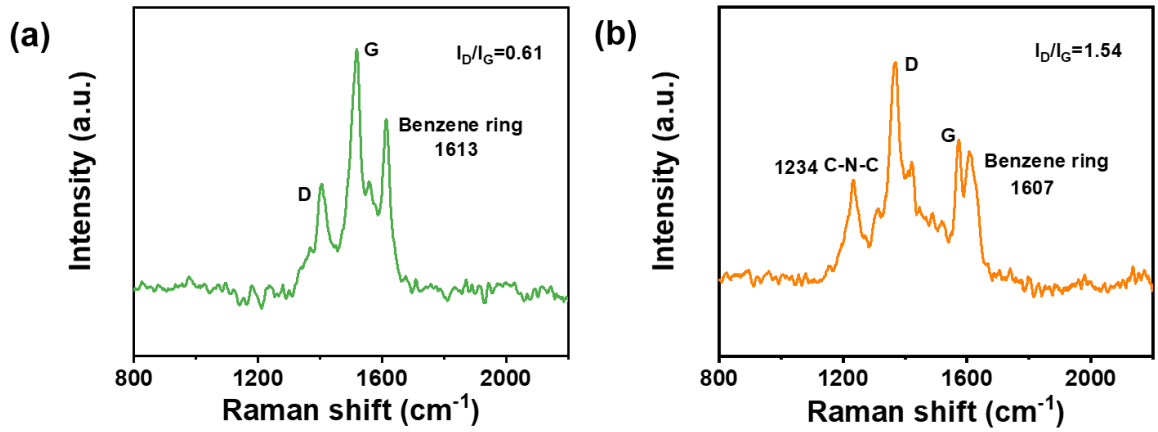

Fig S7 Raman spectra of (a) P3Q and (b) TDB.

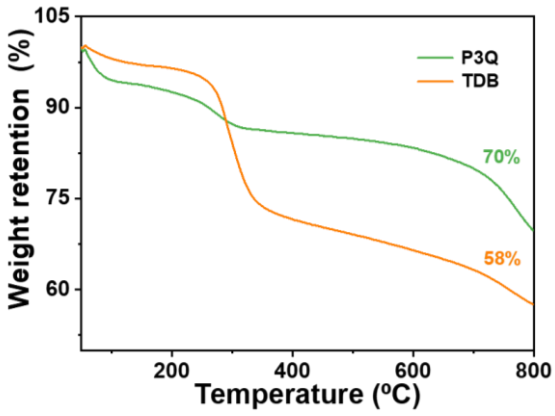

Fig S8 TGA curves of P3Q and TDB.

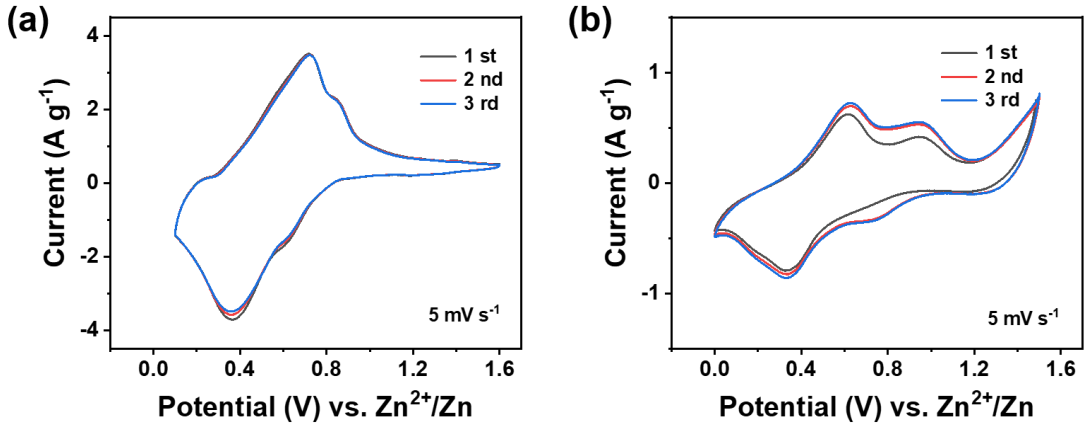

Fig S9 The first three CV curves of (a) P3Q and (b) TDB at 5 mV s^{-1}

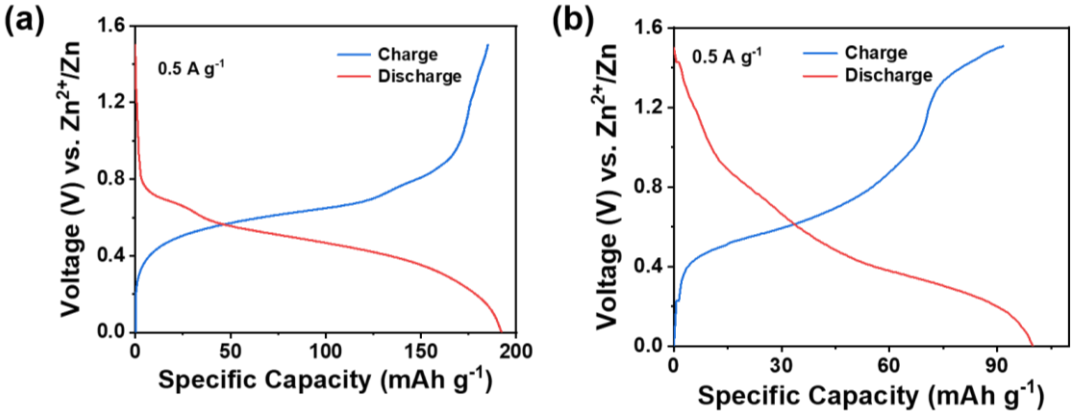

Fig S10 The charge/discharge curves of (a) P3Q and (b) TDB at 0.5 A g^{-1}

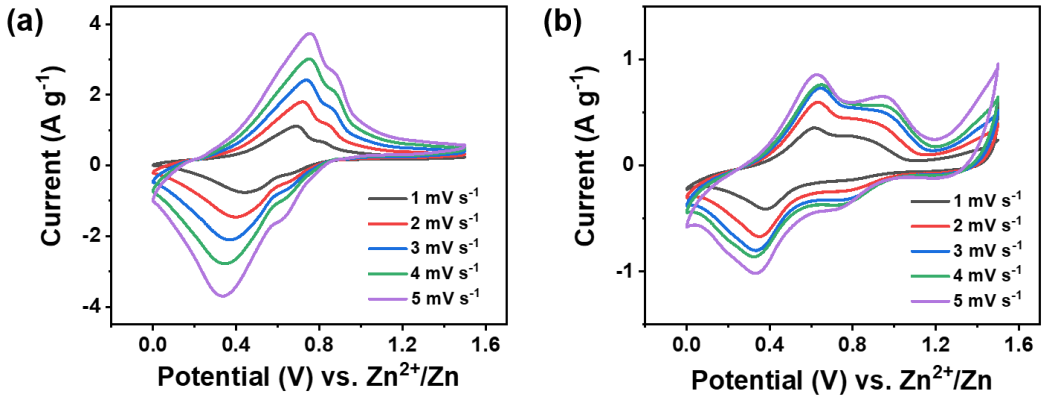

Fig S11 CV curves of (a) P3Q and (b) TDB at various sweep rates in ZIBs.

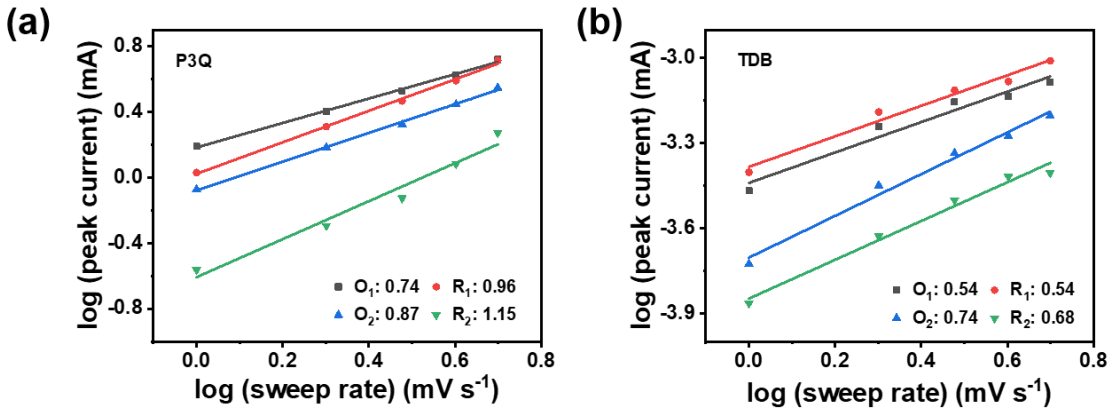

Fig S12 Determination of b value from the logarithm of oxidation/reduction peak current versus logarithm of scan rate for (a) P3Q and (b) TDB.

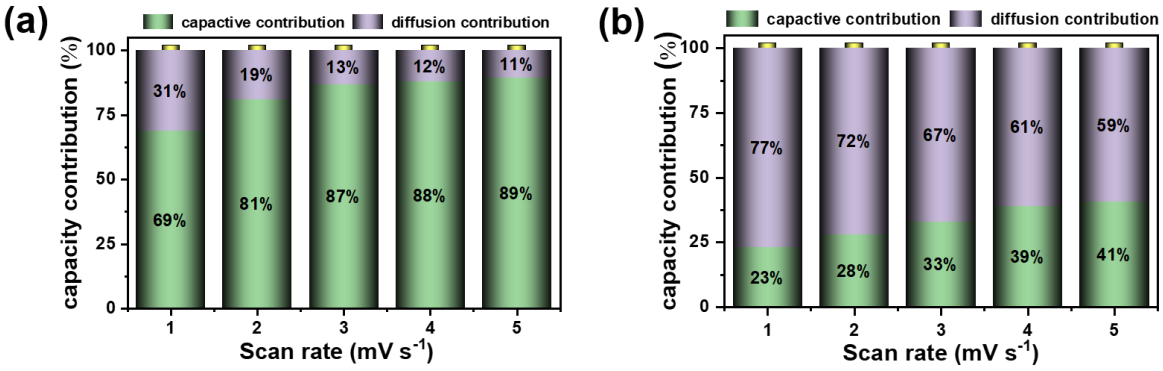

Fig S13 The ratio of capacitance control and diffusion control for (a) P3Q and (b) TDB at different scan rates.

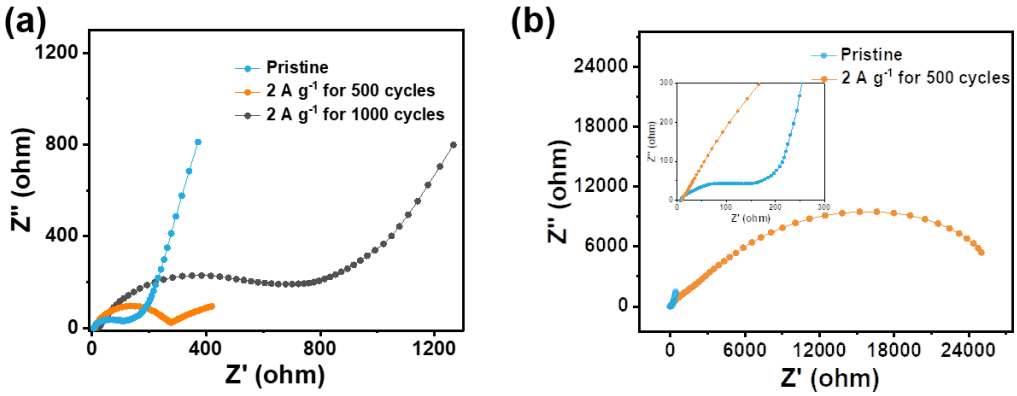

Fig S14 Impedance spectra of (a) P3Q and (b) TDB before and after GCD cycles.

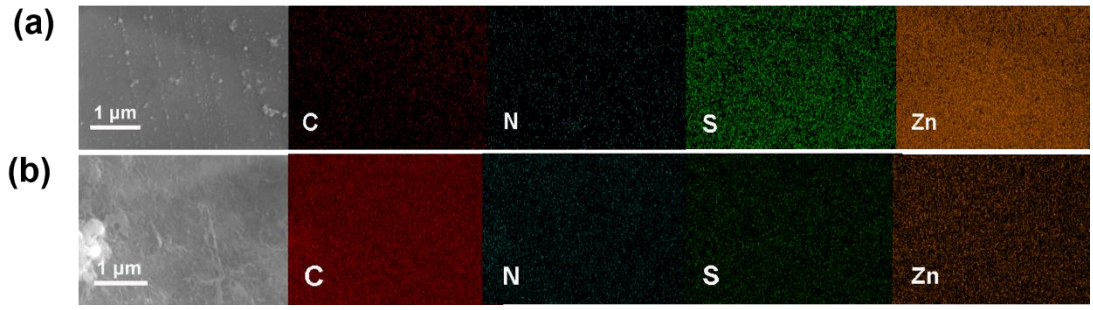

Fig S15 SEM-EDS mapping of C, N, S, and Zn elemental distributions of P3Q electrodes at (a) discharged and (b) charged states at 0.1 A g^{-1}.

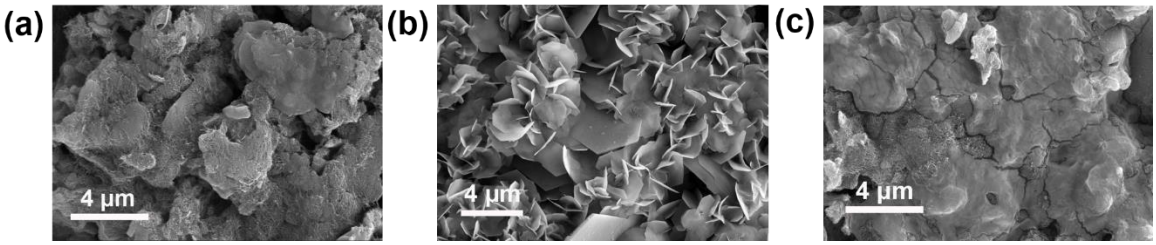

Fig S16 The *ex situ* SEM images of P3Q electrodes at (a) pristine, (b) discharged and (c) charged states at 0.1 A g^{-1}.

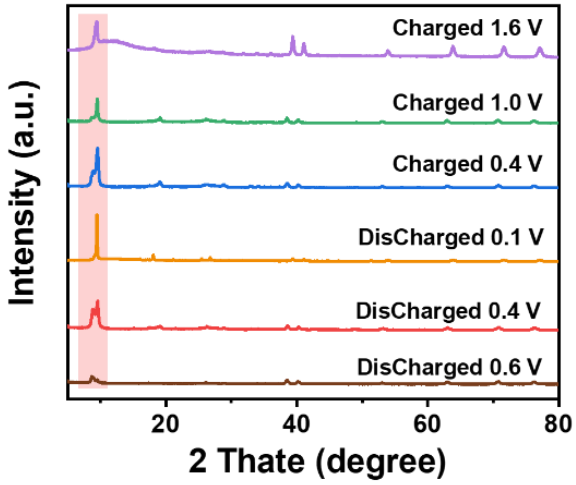

Fig S17 The XRD pattern of P3Q cathode in ZIBs at different GCD states.

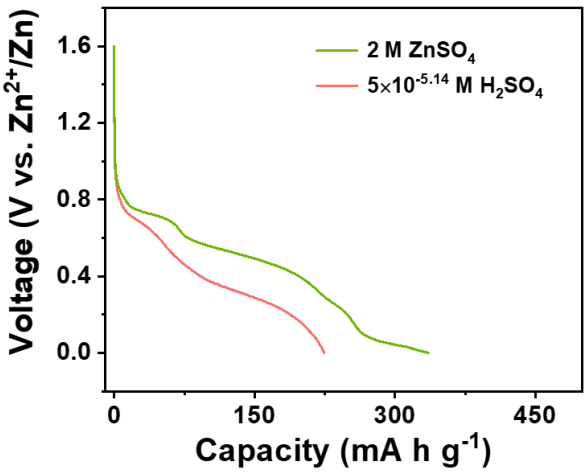

Fig S18 GCD curves at 0.1 A g^{-1} of P3Q in two kinds of electrolytes.

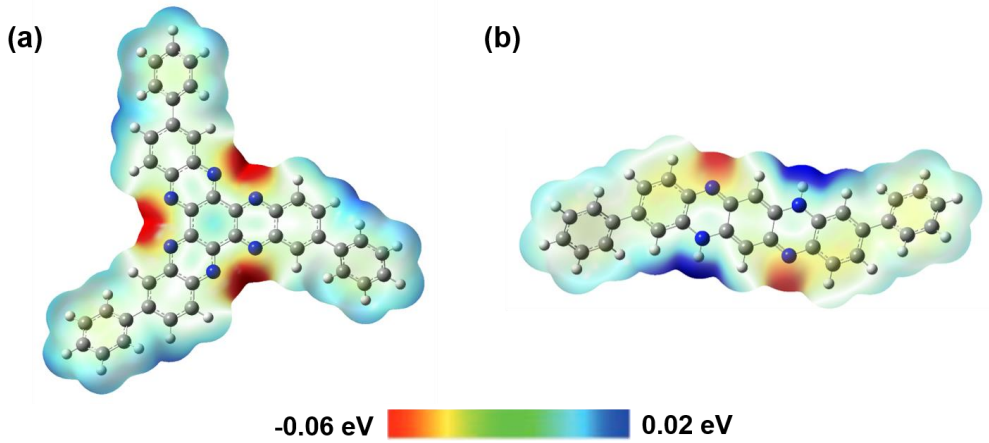

Fig S19 DFT-optimized ESP profiles of (a) P3Q and (b) TDB.

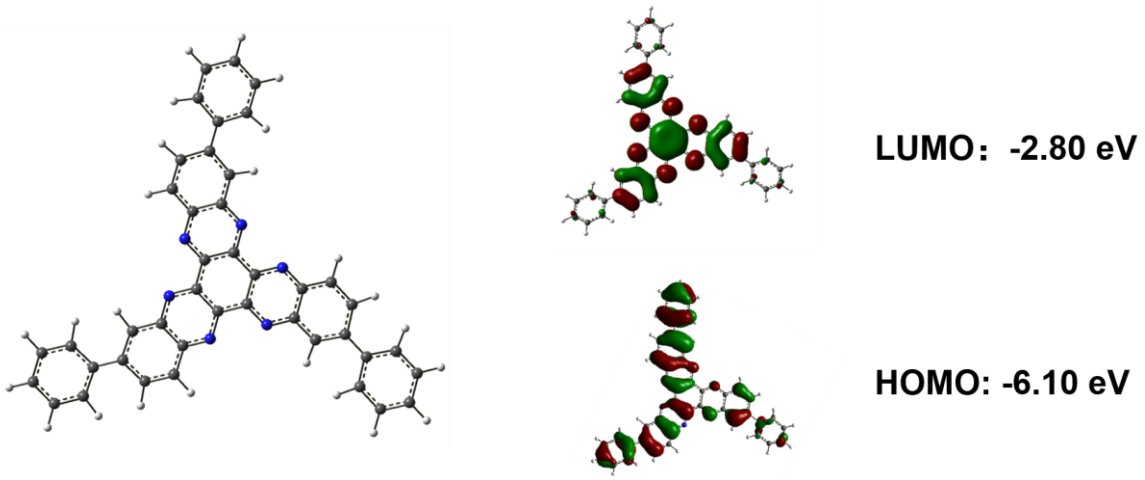

Fig S20 DFT-optimized geometrie, LUMO and HOMO of P3Q.

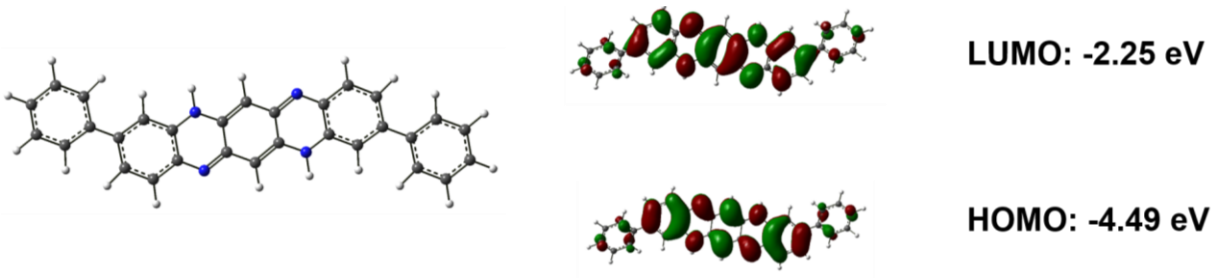

Fig S21 DFT-optimized geometrie, LUMO and HOMO of TDB.

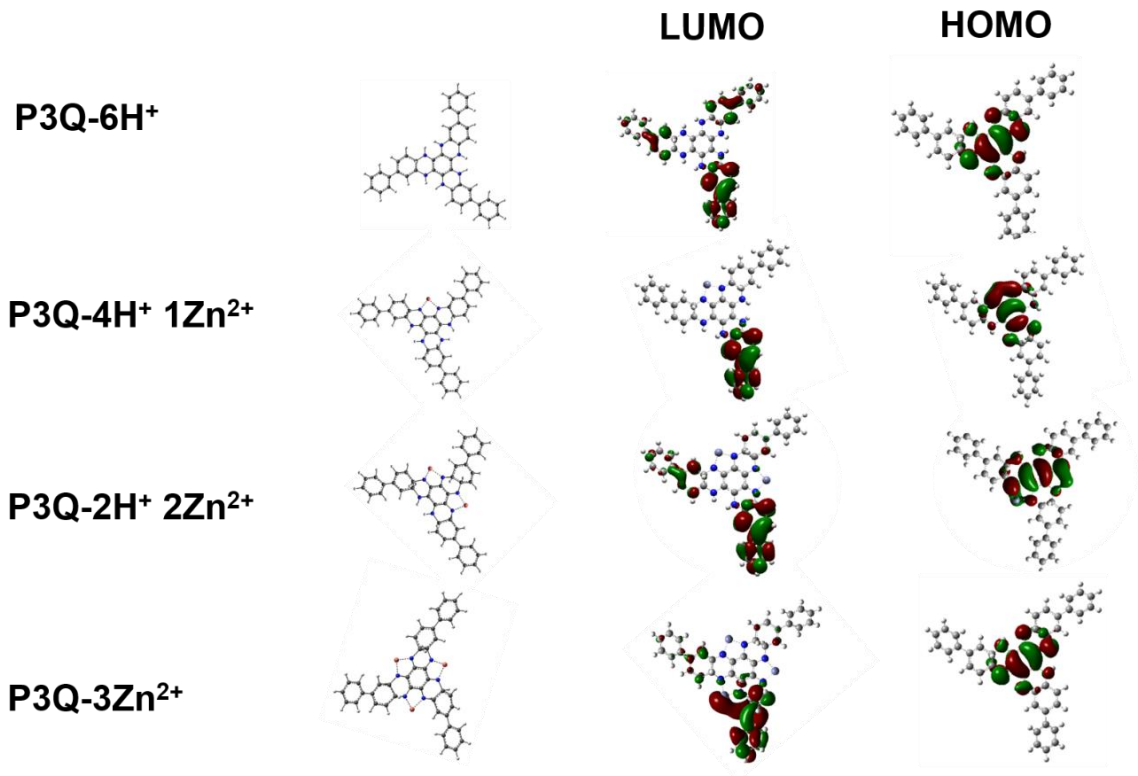

Fig S22 DFT-optimized geometries, LUMOs and HOMOs of P3Q-$6H^+$, P3Q-$4H^+$ $1Zn^{2+}$, P3Q-$2H^+$ $2Zn^{2+}$ and P3Q-$3Zn^{2+}$.